The 8th Pacific Rim International Congress on Advanced Materials and Processing
Edited by: Fernand Marquis
TMS (The Minerals, Metals & Materials Society), 2013

Characterization of the Crystallographic Textures and Mechanical Anisotropy Factors in Two Modifications of Zr-2.5Nb Pressure Tube Materials

Randy Fong[1], Sven Vogel[2], Ron Miller[3], and Henry Saari[3]

[1]Atomic Energy of Canada Limited, Chalk River Laboratories, Chalk River, Ontario, Canada;
[2]Lujan Center, LANSCE, Los Alamos National Laboratory, Los Alamos, New Mexico 87545, U.S.A.;
[3]Department of Mechanical & Aerospace Engineering, Carleton University, Ottawa, Ontario, Canada;
Email: fongr@aecl.ca, sven@lanl.gov, rmiller@mae.carleton.ca, hsaari@mae.carleton.ca

Abstract

Zr-2.5Nb alloy is used for the pressure tubes in CANDU reactors. Current as-manufactured tubes are produced in a cold-worked and stress-relieved metallurgical condition. The tubes installed in reactors normally operate at ~300°C. In a hypothetical loss-of-coolant-accident (LOCA), the pressure tube may be overheated to 1000°C. During the temperature transient, a phase transformation occurs that changes the microstructure and affects the material's high-temperature deformation behaviour. In this study, improvements to enhance the performance of pressure-tube materials are being explored by modifying the texture and microstructure of as-manufactured pressure tubes. Two modifications were carried out by high-temperature annealing, with or without subsequent cold-working. This paper presents the resulting modified textures as measured by neutron diffraction and their texture evolution during heating. The anisotropy factors calculated for the modified Zr-2.5Nb pressure-tube materials using the measured texture data are compared with those previously characterized for Zircaloy-4 fuel cladding. The resulting effect of these texture and microstructure modifications with regard to the material's response to anisotropic deformation during heating to high temperatures is also discussed in this paper.

1. Introduction

The Zr-2.5Nb alloy is used for pressure tube materials in CANDU® reactors. The manufactured tubes are installed in-reactor in a cold-worked and stress-relieved condition. The tubes installed in reactors normally operate at ~300°C. In a hypothetical loss-of-coolant-accident (LOCA), the pressure tube material may be overheated to 1000°C. During the temperature transient, a phase transformation occurs that changes the microstructure and affects the material's high-temperature deformation behaviour.

The pressure tubes are fabricated by the following steps: quadruple melt ingot, forge to bar, machine hollow billets, preheat billets to 815°C and extrude into tubes, cold-draw 25 to 30% (in two wall thickness reductions), and stress relief in steam autoclave for 24 hours at 400°C (which also introduces a protective oxide layer on the inside and outside surfaces of the tube) [1]. The microstructure of as-manufactured pressure tubes typically consists of elongated hexagonal close-packed (hcp) α-Zr grains containing a high dislocation density and a thin layer of body-centered cubic (bcc) β phase at the α-grain boundaries (Fig. 1a and Fig. 1b). At low temperatures (< 610°C), the pressure tubes exhibit a strong transverse crystallographic texture (Fig. 2). During heating to 1050°C, the texture evolution observed in-situ by neutron diffraction was found to be stable [2]. The observed anisotropic deformation of the as-manufactured pressure tube material at high temperatures has been related to the stable evolution of texture during heating. The material's response to the mechanical anisotropy at high temperatures has been ascribed to slips on prism and

---

CANDU® is a registered trademark of Atomic Energy of Canada Limited (AECL).

pyramidal planes in the hcp α-Zr grains, with the deformation at temperatures around 700-750°C being attributed to grain boundary sliding [3].

Improvements on pressure tube materials are constantly being investigated to enhance their property performance in-reactor. For example, the performance of TMT-2 pressure tubes developed for Russian RBMK reactors showed improved crack tolerance after irradiation, and also in-reactor creep which was controlled mostly by texture and its initial microstructure [4]. The research work used alloy powders as starting materials to make the tubes for evaluation [4]. Improvement in delayed hydride cracking is also obtained with radial texture through texture modifications [5-7]. Other evaluations involved pressure tubes made from melted ingots and various thermo-mechanical and cold-working processes [8], including recovery and recrystallization annealing [9]. The evaluations are mostly for low temperature (<500°C) applications of the pressure tube materials. For applications in high temperature deformation, there is little information or evaluation being made on improving the Zr-2.5Nb pressure tube materials.

In this study, two simple modifications (‘A’ and ‘B’) have been made using an as-manufactured Zr-2.5Nb CANDU pressure tube material, to evaluate the modifications of texture and microstructure for improving the high temperature deformation characteristics of the material. The texture of the modified materials and its evolution during heating to 1050°C were evaluated by neutron diffraction at the Los Alamos Neutron Science Center (LANSCE). The texture data were used as input in SELFPOLY (polycrystalline model) to calculate the Kearns (texture) numbers and anisotropy factors to evaluate the material’s high-temperature response to mechanical anisotropy, for some hypothetical LOCA scenarios. Modification ‘A’ material was obtained by applying a high-temperature annealing (875°C for 17 days) on an as-manufactured pressure tube material. Modification ‘B’ was obtained by applying cold-rolling on the Modification ‘A’ material with about 60% cold-work. This paper presents the texture obtained in the two modifications. The texture evolution during high-temperatures heating was found to be stable, similar to the texture evolution observed in as-manufactured pressure tube material [2]. The anisotropy factors calculated are discussed in comparison with those previously determined for Zircaloy-4 fuel sheaths materials [10].

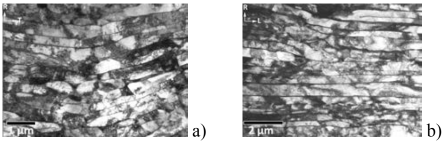

Fig.1 TEM micrographs showing the elongated grain structures of an as-manufactured Zr-2.5Nb pressure-tube material: a) longitudinal-normal direction, and b) transverse-normal direction of the tube

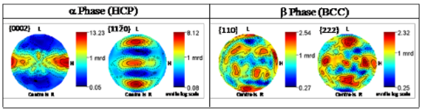

Fig. 2 Pole figures (equal-area-projection) of hcp α- and bcc β-phase in as-manufactured Zr-2.5Nb pressure tube material measured at 100°C [2]

2. Experimental

2.1 Material modifications and sample preparation

Two modifications were performed using an as-manufactured Zr-2.5Nb pressure tube material. The modifications were made using the same pressure-tube material in which the changes in texture and phase transformation during heating to high temperatures and cooling has been previously studied in-situ by neutron diffraction [2]. To prepare the modified materials, two axial slit rings each about 25 mm wide were cut from the as-manufactured pressure tube (Fig. 3). The slit rings were reverse bent obtain a flat strip. After cleaning the flat strip with acetone, each strip was then encapsulated in a quartz tube under vacuum. The two strip materials were then modified, outlined as follows.

- Modification ‘A’ was performed by a high-temperature annealing at 875°C for 17 days and then cooling slowly. The microstructure of the modified material consists of large equiaxed grains of primary α-Zr within a matrix of Widmanstätten α-Zr platelets that were transformed from the prior β-phase, Fig. 4a.

- Modification ‘B’ was performed by cold rolling the Modification ‘A’ material in multi-passes in the same direction along the tube’s transverse direction. A total wall thickness reduction of about 60% was achieved using the rolling mill at CANMET Materials Technology Laboratory. Fig. 4b shows the microstructure of Modification ‘B’ material with elongated grains of primary α-Zr and deformed α-Zr platelets.

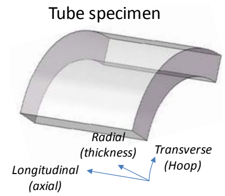

Fig. 3 Three principal directions of tube

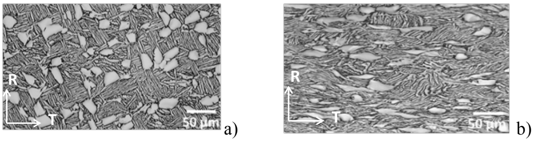

Fig. 4 Optical micrographs showing microstructures of two modified as-manufactured Zr-2.5Nb pressure-tube materials: (a) Modification ‘A’ and (b) Modification ‘B’. (R and T are the radial and transverse direction of the tube, respectively.)

These two modified pressure tube materials were characterized for their texture and evolution during heating to high temperatures up to 1050°C using neutron diffraction. A suitably-sized sample was prepared from each of the two modified materials (Modification ‘A’ and ‘B’).

To increase the sampling volume and thus improve the neutron measurement, the sample was prepared by stacking together two or more plates that were cut from the flat strip of the material (Fig. 5). The overall dimension of the stacked sample is approximately 10 mm tall x 8 mm wide x 8 mm thick. To improve thermal conduction between the two plates, the small curvature and the oxide layer on the surfaces of the plates were mechanically polished, then cleaned with acetone and the plates held tightly stacked together by spot-welding on a thin Zr-foil on both sides of the stacked sample. The neutron scattering from the thin Zr foils is expected to be minor since the volume of the stacked sample (volume being probed) is much larger than that of the foil, and hence they would not significantly alter the diffraction profile obtained from the stacked sample.

Fig. 5 A schematic diagram showing a stacked sample consisting of two plates taken from the Zr-2.5Nb pressure tube material. The hoop direction of the sample is aligned with the furnace axis of rotation. The plates are held tightly together by spot-welded Zr-foils (not shown in the diagram).

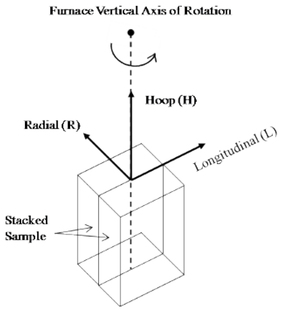

2.2 Neutron diffraction measurements

Neutron diffraction measurements for texture were made on the two modifications ('A' and 'B') of Zr-2.5Nb pressure tube materials. The texture measurements were performed on the time-of-flight (TOF) high-pressure preferred orientation (HIPPO) diffractometer at LANSCE. The details for such TOF texture measurements can be found in [2]. To perform the measurements, the sample is placed in a vanadium basket inside a vacuum furnace with vanadium heating elements and heat shields. An incident beam of polychromatic thermal neutrons collimated to 10 mm beam diameter was directed at the sample. Two thermocouples are located in the furnace at about 70 mm above the sample within the 200-mm high hot zone, with one used to control and record the temperature of the sample. The uncertainty in the sample temperature for the furnace used in this study is estimated to be less than ±5°C.

The pole figures of α and β phases were measured during heating of the sample at eight different temperatures (100°C to 1050°C), traversing across the two solvus lines along the Zr-2.5Nb composition [11]. At each temperature, the sample was rotated around the furnace axis in three different rotations (0°, 45° and 90°). Diffraction data were collected at each of the three rotations for a period of 18 minutes which was deemed sufficient to obtain the ODF (orientation distribution function) of the crystallites in the sample to reconstruct pole figures for many different planes. The total time for each temperature interval was about 1 h. The pole intensities measured with three panels of detectors were used to extract texture information using the Rietveld method, as implemented in the MAUD program [12] for analyzing HIPPO diffraction data. The ODF is calculated using the EWIMV algorithm, as implemented in MAUD that allows data to be entered at arbitrary pole figure positions [13-15]. A 10° x 10° x 10° grid was used for calculating the ODF in the sample for each test temperature. No sample symmetry was imposed on the calculations. The complete pole figures for both α and β phases were reconstructed using the calculated ODFs. In this paper, all the reconstructed pole figures are represented on a Lambert equal-area projection [16], and the ODF plots are only presented for heating at 100°C and 900°C to provide clarity for discussion. The ODF data were used as input in SELFPOLY [17-18], to calculate the Kearns (texture) numbers [19] and Hill's anisotropy factors [20].

2.3 Kearns numbers and Hill's anisotropy factors

2.3.1 Kearns numbers

The Kearns numbers [19] for the three principal directions in the sample (f_R, f_T, and f_L), defined as a weighted average of the intensity of the basal plane normals oriented with respect to the sample's principal direction, are calculated using eqn. (1).

$$f_d = \left[\sum_{\alpha_d} V_f(\alpha_d, \beta) sin\alpha_d cos^2\alpha_d\right] / \left[\sum_{\alpha_d} V_f(\alpha_d, \beta) sin\alpha_d\right] \qquad (1)$$

Here d stands for R (radial), T (transverse) and L (longitudinal) direction of the original tube sample. $V_f(\alpha_d, \beta)$ is the volume fraction of grains with basal poles oriented at a given polar and azimuthal angles α_d and β in the pole figure for the sample, respectively. Normally, the sum of the three Kearns numbers must equal to 1 (eqn. 2).

$$f_R + f_T + f_L = 1 \qquad (2)$$

The calculated Kearns numbers for the modified ('A' and 'B') materials are compared with those of as-manufactured pressure tube [16], summarized in Table 1.

2.3.2 Hill's anisotropy factors [20]

Hill [20] first proposed a theory of yielding of anisotropic metals by modification of the Huber-Hencky von Mises isotropic yielding with three tensile anisotropic factors designated as F, G, and H. In Cartesian co-ordinates (θ = transverse, z = longitudinal, and r = radial), and for loading only in the principal directions of a tube, the Hill's yield criterion is defined, in terms of the Huber-von Mises equivalent stress, as

$$\bar{\sigma} = [F(\sigma_\theta - \sigma_z)^2 + G(\sigma_z - \sigma_r)^2 \ + H(\sigma_r - \sigma_\theta)^2]^{½} \tag{3}$$

The onset of yielding occurs when $\bar{\sigma} = Y$. The Hill's anisotropy factors for the two modified pressure tube materials were calculated using SELFPOLY model [18] with the measured texture (ODF) data as input for the calculations. The SELFPOLY model is a self-consistent polycrystalline model that has been developed to predict the deformation of polycrystals by averaging the behaviour of individual crystals and by assuming a certain deformation mechanism at the single crystal level [17]. Later, Turner el al [18] included a model for thermal creep by adopting Hutchinson's slip [23] models for power-law steady state creep of polycrystals. In the SELFPOLY model [18], the single-crystal deformation rate is given by

$$\dot{\varepsilon}_{ij} \ = \textstyle\sum_s \dot{\gamma}_0^s \left(\frac{m^s:\sigma}{\tau^s}\right)^n m_{ij}^s \tag{4}$$

Here, σ is the deviatoric stress acting on the crystal, the index *s* stands for the slip system (e.g., prismatic slip (τ^{pr}), basal slip (τ^{bas}) or pyramidal slip (τ^{pyr}), the tensor m_{ij}^s is the Schmid tensor corresponding to the slip system s, and, for each slip system, τ^s and $\dot{\gamma}_0^s$ are the CRSS (i.e., critical resolved shear stress) and the reference shear strain rate, respectively. The stress exponent (*n*) is the inverse of the strain-rate sensitivity, i.e., $n = 1/m$. Details for this formulation are described in [24]. Pang et al. [25] fitted the tensile loading curves for Zircaloy-2 material under uniaxial deformation and determined suitable parameters for the three slip modes (PR = prismatic, BAS = basal, and PYR = pyramidal), and they found that the CRSS values were 90 MPa for PR, 160 MPa for BAS and 240 MPa for PYR, giving a CRSS ratio of 1:1.8:2.7 (a ratio of prismatic to basal to pyramidal).

In this analysis, SELFPOLY is used to calculate the Hill's anisotropy factors using the fixed value for the CRSS ratio from Pang et al. [25] and the value for the stress-exponent *n* is obtained through use of a texture-based parameter, ζ given as

$$\zeta = n = \frac{f_T}{f_L} + (+(f_R - f_T)^2 + \ (f_T - f_L)^2 f_R - f_L)^2 \tag{5}$$

where *n* is the stress exponent parameter used in SELFPOLY (eqn. (4)), and f_R, f_T, f_L, are the Kearns numbers defined in eqn. (1). The method of analysis used in this work is essentially the same as that used previously to calculate the anisotropy factors of fuel sheaths using measured texture data [10]. The anisotropy factors calculated for the modified ('A' and 'B') materials are compared with those of as-manufactured pressure tube [16] material, and are summarized as shown in Table 1.

Table 1. Kearns numbers and Hill's anisotropy factors calculated using ODF data from hcp α-Zr phase obtained by neutron diffraction

Zr-2.5Nb pressure-tube material	Kearns numbers			Hill's anisotropy factors		
	f_R	f_T	f_L	F	G	H
As-manufactured	0.26	0.61	0.13	1.03	0.34	0.13
Modification 'A'	0.18	0.38	0.45	0.53	0.44	0.53
Modification 'B'	0.21	0.13	0.66	0.83	0.18	0.49

3. Results and Discussion

3.1 *Pole figures of modifications ('A' and 'B') of Zr-2.5Nb pressure tube materials*

Fig. 6 shows a comparison of the pole figures of hcp α-phase and bcc β-phase for the Modification 'A' and 'B' materials measured during heating up to 1050°C. The pole figures measured at intermediate heating temperatures between 100 and 800°C are not shown since they are the same as those at 800°C. Examination of the pole figures for the α-phase in the two modified materials suggests that the texture on heating to 800°C remained unchanged, thus the texture evolution is deemed to be stable. This observation of stable texture evolution is consistent with that previously observed in as-manufactured Zr-2.5Nb pressure tube materials [2]. With a stable texture evolution, the response to mechanical anisotropy during high temperature deformation can be expected to remain unchanged since the α-phase material would be responsible for most of the deformation. As shown in a previous study [3], the anisotropy in high-temperature deformation is also influenced by grain boundary sliding, as a result of different volume fractions of β-phase present in the material during the α→β phase transformation that occur on heating.

On further heating to 900°C, a new α-phase texture component appears distinctly (indicated by the red arrows shown in Fig. 6 for the Modification ‘A’ material). In comparison, the Modification ‘B’ material also shows the same α-texture component appearing but with a lower intensity. The appearance of this texture component is due to coarsening of the prior “primary” α-Zr grains that were initially present in the two modified materials (Fig. 4). This has also been previously observed in as-manufactured pressure tube [2]. The evolution of α-phase texture resulting from the transformation of Widmanstätten α-platelets to β-phase material, and the coarsening of the prior primary α-Zr grains during heating, are clearly revealed in the ODF plots shown in Fig. 7, and discussed in Section 3.2.

Examination of the transformed β-phase in Modification ‘A’ material on heating up to 1050°C (full β-phase field), Fig. 6, shows that the β-phase texture remained unchanged throughout the entire heat-up schedule. This β-phase texture evolution is deemed to be a stable transformation process. In comparison, the texture evolution of transformed β-phase in Modification ‘B’ material remained unchanged on heating only up to 900°C (Fig. 6). However, on further heating to 1050°C the β-phase texture had evolved to be different from that observed at 900°C.

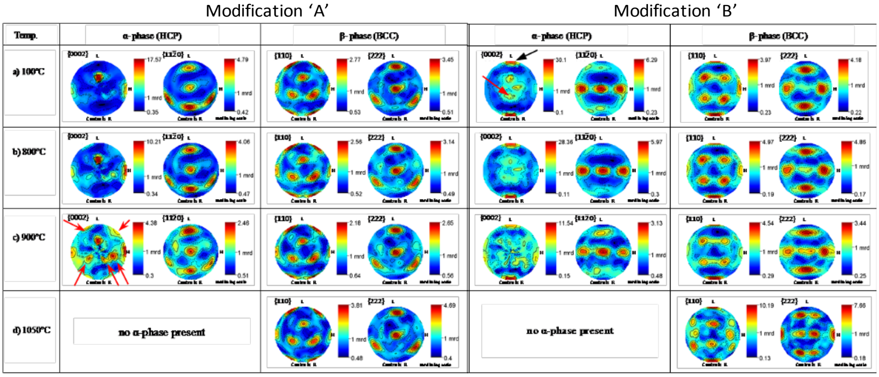

Fig. 6 Pole figures (equal-area projection) of Modification ‘A’ and Modification ‘B’ of Zr-2.5Nb pressure tube material on heating up to 1050°C

3.2 *ODF plots of hcp α-phase in measured samples at 100°C and 900°C*

Fig. 7 shows the ODFs of hcp α-phase in the as-manufactured and two modifications (‘A’ and ‘B’) of Zr-2.5Nb pressure tube materials that were measured at 100°C and 900°C on heating. Examination of the ODFs at 100°C, shows that the as-manufactured material initially has three different texture components (labelled A, B, and C in the figure) with a pronounced a transverse texture (label B). By applying a high-temperature annealing treatment to obtain the Modification ‘A’ material, the phase transformation processes that occurred during heating to 875°C for 17 days and slowly cooling back to room temperature have resulted in two almost equally pronounced texture components (labelled C and D). Using the diagram (Fig. 7) as a guide to illustrate the crystal orientations in relation to the sample axes, it is shown that the basal poles for the two texture components discussed earlier, are basically aligned with the transverse and close to the longitudinal direction of the tube. Modification ‘B’ material is produced by applying cold rolling on the Modification ‘A” material. The process of cold rolling applied along the tube’s transverse direction can produce twinning in the grains to generate the two visibly new texture components (labelled E and F) with basal poles aligned along the tube’s longitudinal and radial direction. In the ODF plot, there is a relocation of texture component from one of the initial two texture components (labelled C) to two new locations (labelled E and F), resulting in reducing the ODF intensity of that particular texture component (labelled H). This observation suggests that cold rolling along the transverse direction of the tube induces twinning to be produced only in grains with the prior transverse texture component.

At 900°C on heating, previously unobserved α-phase texture components appeared for all the three materials. As previously reported for as-manufactured pressure tube [2], the appearance of these texture components (labelled I and J) was a result of the coarsening of the prior ‘primary’ α-Zr grains. The coarsening process is also responsible for the additional texture components observed in Modification ‘A’ material (labelled K and L). Similarly, additional texture components were also observed in Modification ‘B’ material (labelled N).

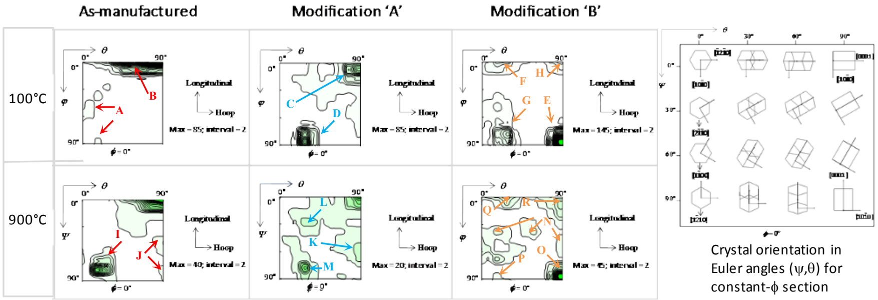

Fig. 7 ODF plots (for ϕ=0°) of hcp α-phase in as-manufactured Zr-2.5Nb pressure tube and two modifications (’A’ and ‘B’) of pressure tube materials on heating at 100°C and 900°C. (Insert on the right hand side is an illustration showing different crystal orientations described by Euler angles (ψ,θ) for constant-ϕ section)

3.2 Comparison of yield loci using Hill’s criterion

Using the calculated Hill’s anisotropy factors (*F*, *G* and *H* values listed in Table 1), a yield locus is generated using Hill’s criterion (eqn. (3)) for a biaxial stress state for the pressure tube materials, as shown in Fig. 8. For comparison, the yield loci previously produced for Zircaloy-4 fuel sheath materials [10] are also included in the same figure. A larger size of an ellipse (i.e., yield locus) indicates a stronger anisotropy in yielding behaviour that can be expected when the tubing material is stressed biaxially.

In Fig. 8, for pressure tube materials, the mechanical anisotropy is strongest in an as-manufactured pressure tube, compared to the two modified materials (‘A’ and ‘B’). Annealing in Modification ‘A’ gave almost isotropic property, and the cold rolling made on Modification ‘A’ material increased the size of the ellipse, making it more anisotropic but not so anisotropic as the as-manufactured pressure tube. The transverse rolling generated a stronger axial (longitudinal) direction for yielding.

In comparison, the Zircaloy-4 fuel sheath with un-brazed material shows a yield anisotropy response similar in size to the Modification ‘B’ material (their ellipses are about the same size), but has a stronger transverse direction. The simulated brazed fuel sheath [10] shows similar isotropy as that in Modification ‘A’ material since both these materials had gone through a high-temperature anneal.

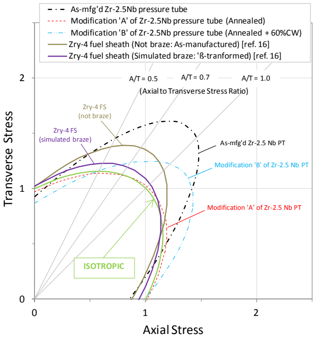

Fig. 8 A comparison of anisotropic yield loci of Zr-2.5Nb pressure tube materials (as-manufactured, Modification ‘A’ and Modification ‘B’) and Zircaloy-4 fuel sheath materials (as-fabricated, and simulated braze microstructure)

4. Conclusions

The following conclusions are drawn from this study.

1. Modification ‘A’, a high-temperature annealing process applied on as-manufactured Zr-2.5Nb pressure tube, has been shown to modify its initial pronounced transverse texture and to produce a dual-textured material with basal poles aligned in the transverse and longitudinal directions of the tube. Although being dual-textured, the material shows an isotropic property.
2. Modification ‘B’, an application of cold-rolling process on a dual-textured material (Modification ‘A”), is shown to produce further texture modifications, resulting in a quad-textured material with an anisotropic property stronger in the axial (i.e., longitudinal) direction of the tube.
3. The texture evolution in the two modified materials appeared to be stable during heating up to 900°C.

References

[1] B.A. Cheadle, *J. ASTM International*, Vol. 7, No. 8, Paper ID JAI103057, 2010
[2] R.W.L. Fong, R. Miller, H.J. Saari and S.C. Vogel, *Metall. Mater. Trans A*, Vol. 43A, pp. 806-821, 2012
[3] R.W.L. Fong, (*in Press)*, *J. Nucl. Mater*., 2013
[4] C. Coleman, et al., *J. ASTM International*, Vol. 4, No. 10, Paper ID JAI1101111, 2007
[5] S.S. Kim and Y.S. Kim, *J. Nucl. Mater*., Vol. 279, pp. 286-292, 2000
[6] C.E. Coleman, S. Sagat and K.F. Amouzouvi, 26th Ann. Conf. Metall., CIM, Winnipeg, Manitoba, 1987
[7] C.E. Coleman, et al., Zirconium in the Nuclear Industry, *ASTM STP 1295*, pp. 884–898, 1996
[8] N. Saibaba, et al., *J. ASTM International*, Vol. 8, No. 6, Paper ID JAI103213, 2011
[9] V.D. Hiwarkar, et al., *J. Nucl. Mater*., Vol. 384, pp. 30-37, 2009
[10] R.W.L. Fong, (*Accepted for Publication)*, *J. Nucl. Mater*., 2013
[11] J.P. Abriata and J.C. Bolcich, *Bull. Alloy Phase Diagrams*, Vol. 3, No. 1, pp. 34-44, 1982
[12] H.R. Wenk, L. Lutterotti and S.C. Vogel, *J. Powder Diffraction*, Vol. 25, No. 3 (14 pp.), 2010
[13] S. Matthies, L. Lutterotti and H.R. Wenk, *J. Appl. Crystallogr*. 30: 31–42, 1997
[14] S. Matthies, et al., *J. Appl. Crystallogr*. 38:462–475, 2005.
[15] L. Lutterotti, et al., Thin Solid Films, 450:34, 2004
[16] H.R. Wenk, Academic Press, pp. 11-14, 1985
[17] C.N. Tomé, C.B. So, and C.H. Woo, *Phil. Mag.* A 67, pp. 917-930, 1993
[18] P.A. Turner, et al., *Phil. Mag. A*, vol. 79(10), pp. 2505-2524, 1999
[19] J.J. Kearns, Thermal expansion and preferred orientation in Zircaloy, WAPD-TM-472, 1965
[20] R. Hill, *Proc. Roy. Soc. A*, 193, London, p. 281, 1948
[21] C.E.L. Hunt, 3rd Int. Conf. Struct. Mech. Reactor Techn., London, U.K., Vol. 1, Paper C 2/9, 1-5 Sept., 1975
[22] C.E.L. Hunt and W.G. Newell, Zirconium in the Nuclear Industry, *ASTM STP 681*, pp. 447-464, 1979
[23] J.W. Hutchinson, *Proc. Roy. Soc., Lond*., A348, pp. 101-127, 1976
[24] N. Christodoulou, et al., *Metall. Mater. Trans. A*, Vol. 31A, pp. 409-420, 2000
[25] J.W.L. Pang, T.M. Holden, P.A. Turner, and T.E. Mason, *Acta Mater*., Vol. 47 (2), pp. 373-383, 1999